

NEW FRONTIERS IN ASYMMETRIC CATALYSIS

Edited by

KOICHI MIKAMI

Department of Applied Chemistry, Tokyo Institute of Technology

MARK LAUTENS

Department of Chemistry, University of Toronto



WILEY-INTERSCIENCE

A JOHN WILEY & SONS, INC., PUBLICATION

**NEW FRONTIERS
IN ASYMMETRIC
CATALYSIS**



THE WILEY BICENTENNIAL—KNOWLEDGE FOR GENERATIONS

Each generation has its unique needs and aspirations. When Charles Wiley first opened his small printing shop in lower Manhattan in 1807, it was a generation of boundless potential searching for an identity. And we were there, helping to define a new American literary tradition. Over half a century later, in the midst of the Second Industrial Revolution, it was a generation focused on building the future. Once again, we were there, supplying the critical scientific, technical, and engineering knowledge that helped frame the world. Throughout the 20th Century, and into the new millennium, nations began to reach out beyond their own borders and a new international community was born. Wiley was there, expanding its operations around the world to enable a global exchange of ideas, opinions, and know-how.

For 200 years, Wiley has been an integral part of each generation's journey, enabling the flow of information and understanding necessary to meet their needs and fulfill their aspirations. Today, bold new technologies are changing the way we live and learn. Wiley will be there, providing you the must-have knowledge you need to imagine new worlds, new possibilities, and new opportunities.

Generations come and go, but you can always count on Wiley to provide you the knowledge you need, when and where you need it!

William J. Pesce *Peter Booth Wiley*

WILLIAM J. PESCE
PRESIDENT AND CHIEF EXECUTIVE OFFICER

PETER BOOTH WILEY
CHAIRMAN OF THE BOARD

NEW FRONTIERS IN ASYMMETRIC CATALYSIS

Edited by

KOICHI MIKAMI

Department of Applied Chemistry, Tokyo Institute of Technology

MARK LAUTENS

Department of Chemistry, University of Toronto



WILEY-INTERSCIENCE

A JOHN WILEY & SONS, INC., PUBLICATION

Copyright © 2007 by John Wiley & Sons, Inc. All rights reserved.

Published by John Wiley & Sons, Inc., Hoboken, New Jersey
Published simultaneously in Canada

No part of this publication may be reproduced, stored in a retrieval system, or transmitted in any form or by any means, electronic, mechanical, photocopying, recording, scanning, or otherwise, except as permitted under Section 107 or 108 of the 1976 United States Copyright Act, without either the prior written permission of the Publisher, or authorization through payment of the appropriate per-copy fee to the Copyright Clearance Center, Inc., 222 Rosewood Drive, Danvers, MA 01923, 978-750-8400, fax 978-750-4470, or on the web at www.copyright.com. Requests to the Publisher for permission should be addressed to the Permissions Department, John Wiley & Sons, Inc., 111 River Street, Hoboken, NJ 07030, 201-748-6011, fax 201-748-6008, or online at <http://www.wiley.com/go/permission>.

Limit of Liability/Disclaimer of Warranty: While the publisher and author have used their best efforts in preparing this book, they make no representations or warranties with respect to the accuracy or completeness of the contents of this book and specifically disclaim any implied warranties of merchantability or fitness for a particular purpose. No warranty may be created or extended by sales representatives or written sales materials. The advice and strategies contained herein may not be suitable for your situation. You should consult with a professional where appropriate. Neither the publisher nor author shall be liable for any loss of profit or any other commercial damages, including but not limited to special, incidental, consequential, or other damages.

For general information on our other products and services or for technical support, please contact our Customer Care Department within the United States at 877-762-2974, outside the United States at 317-572-3993 or fax 317-572-4002.

Wiley also publishes its books in a variety of electronic formats. Some content that appears in print may not be available in electronic formats. For more information about Wiley products, visit our web site at www.wiley.com.

Wiley Bicentennial Logo: Richard J. Pacifico

Library of Congress Cataloging-in-Publication Data:

New frontiers in asymmetric catalysis / edited by Koichi Mikami and Mark Lautens.

p. cm.

Includes bibliographical references and index.

978-0-471-68026-0

1. Catalysis—Research. 2. Asymmetry (Chemistry)—Research. I. Mikami, Koichi. II. Lautens, M. (Mark)

QD505.N474 2007

541'.395- -dc22

2006020555

Printed in the United States of America

10 9 8 7 6 5 4 3 2 1

CONTENTS

PREFACE	xi
CONTRIBUTORS	xv
1 Ligand Design for Catalytic Asymmetric Reduction	1
<i>Takeshi Ohkuma, Masato Kitamura, and Ryoji Noyori</i>	
1.1 Introduction	1
1.2 Hydrogenation of Olefins	2
1.2.1 Enamide Hydrogenation with Rhodium Catalysts	2
1.2.2 Hydrogenation of Functionalized Olefins with Ruthenium Catalysts	9
1.2.3 Hydrogenation of Simple Olefins with Iridium Catalysts	11
1.3 Reduction of Ketones	12
1.3.1 Hydrogenation of Functionalized Ketones	12
1.3.2 Hydrogenation of Simple Ketones	15
1.3.3 Transfer Hydrogenation of Ketones	20
1.3.4 Hydroboration of Ketones	22
1.4 Reduction of Imines	25
References	28
2 Ligand Design for Oxidation	33
<i>Tohru Yamada</i>	
2.1 Introduction	33
2.2 Catalytic Enantioselective Epoxidation of Unfunctionalized Olefins	35

2.3	Enantioselective Metal-Catalyzed Baeyer–Villiger Oxidation	44
2.4	Optical Resolution during Oxidation of Alcohols	48
2.5	Catalytic Enantioselective Oxidative Coupling of 2-Naphthols	50
2.6	Concluding Remarks	55
	References	55
3	Ligand Design for C–C Bond Formation	59
	<i>Ryo Shintani and Tamio Hayashi</i>	
3.1	Introduction	59
3.2	1,4-Addition and Related Reactions	59
3.2.1	Copper Catalysis	60
3.2.2	Rhodium Catalysis	69
3.3	Cross-Coupling Reactions	89
3.3.1	Kumada-Type Cross-Couplings	90
3.3.2	Suzuki-Type Cross-Couplings	96
	References	97
4	Activation of Small Molecules (C=O, HCN, RN=C, and CO₂)	101
	<i>Kyoko Nozaki</i>	
4.1	Introduction	101
4.2	Asymmetric Hydroformylation of Olefins	102
4.2.1	The Mechanism of Hydroformylation	103
4.2.2	Scope and Limitation of Asymmetric Hydroformylation	104
4.2.3	“Greener” Catalysts in Asymmetric Hydroformylation	111
4.3	Asymmetric Hydrocarbohydroxylation and Related Reactions	112
4.3.1	Asymmetric Hydrocarbalkoxylation of Alkenes	112
4.3.2	Asymmetric Oxidative Hydrocarbalkoxylation of Alkenes	112
4.3.3	Asymmetric Carbonylation of Carbon–Heteroatom Bonds	115
4.4	Asymmetric Ketone Formation from Carbon–Carbon Multiple Bonds and CO	115
4.4.1	Asymmetric Pauson–Khand Reaction	115
4.4.2	Asymmetric Alternating Copolymerization of Olefins with CO	118
4.4.3	Asymmetric Polymerization of Isocyanide	118
4.5	Asymmetric Hydrocyanation of Olefins	119
4.6	Asymmetric Addition of Cyanide and Isocyanide to Aldehydes or Imines	120
4.7	Asymmetric Addition of Carbon Dioxide	123
4.8	Conclusion and Outlook	124
	References	124
5	Asymmetric Synthesis Based on Catalytic Activation of C–H Bonds and C–C Bonds	129
	<i>Zhiping Li and Chao-Jun Li</i>	
5.1	Introduction	129

5.2	Asymmetric Synthesis via Activation of C–H Bonds	130
5.2.1	Formation of C–C Bonds	130
5.2.2	Formation of C–O Bonds	142
5.2.3	Formation of C–N Bonds	144
5.3	Asymmetric Synthesis via Activation of C–C Bonds	145
5.3.1	Enantioselective C–C Bond Cleavage	146
5.3.2	Formation of C–C Bonds	146
5.3.3	Formation of C–O Bonds	149
5.4	Conclusions and Outlook	149
	Acknowledgments	150
	References	150
6	Recent Progress in the Metathesis Reaction	153
	<i>Miwako Mori</i>	
6.1	Introduction	153
6.2	Olefin Metathesis	155
6.2.1	Ring-Closing Olefin Metathesis	155
6.2.2	Cross-Metathesis (CM) of Diene	165
6.2.3	Ring-Opening Metathesis (ROM)–Ring-Closing Metathesis (RCM) of Alkene	167
6.2.4	Catalytic Asymmetric Olefin Metathesis	173
6.3	Enyne Metathesis	182
6.3.1	Ring-Closing Enyne Metathesis	182
6.3.2	Ring-Opening Metathesis (ROM)–Ring-Closing Metathesis (RCM) of Cycloalkene-Yne	186
6.3.3	Dienyne Metathesis	190
6.3.4	Cross-Metathesis of Enyne	193
6.4	Alkyne Metathesis	196
6.5	Conclusions	202
	References	203
7	Nonlinear Effects in Asymmetric Catalysis	207
	<i>Henri B. Kagan</i>	
7.1	Introduction	207
7.2	Properties of Enantiomer Mixtures	208
7.2.1	Physical Properties	208
7.2.2	Chemical Properties	208
7.3	Nonlinear Effect in Asymmetric Catalysis	209
7.3.1	The First Evidences	209
7.3.2	Origin of Nonlinear Effects: Some Models	210
7.4	Main Classes of Reactions	212
7.4.1	Organometallic Catalysts	213
7.4.2	Organocatalysts	213
7.5	Asymmetric Amplification	213

7.6	Current Trends	216
7.7	Conclusion	216
	Acknowledgment	216
	References and Notes	217
8	Asymmetric Activation and Deactivation of Racemic Catalysts	221
	<i>Koichi Mikami and Kohsuke Aikawa</i>	
8.1	Introduction	221
8.2	Racemic Catalysis	222
8.2.1	Asymmetric Deactivation	223
8.2.2	Asymmetric Activation of Chirally Rigid (Atropos) Catalysts	228
8.2.3	Asymmetric Activation/Deactivation of Chirally Rigid (Atropos) Catalysts	238
8.2.4	Self-Assembly into the Most Enantioselective Catalyst	239
8.2.5	Asymmetric Activation of Chirally Flexible (Tropos) Catalysts	243
8.3	Future Perspectives	254
	References and Notes	255
9	Asymmetric Autocatalysis with Amplification of Chirality and Origin of Chiral Homogeneity of Biomolecules	259
	<i>Kenso Soai, Tsuneomi Kawasaki, and Itaru Sato</i>	
9.1	Introduction	259
9.2	Asymmetric Autocatalysis	260
9.3	Amplification of Chirality by Asymmetric Autocatalysis	262
9.4	Asymmetric Autocatalysis and Its Role in the Origin and Amplification of Chirality	263
9.4.1	Asymmetric Autocatalysis Triggered by Organic Compounds Induced by Circularly Polarized Light	263
9.4.2	Asymmetric Autocatalysis Triggered Directly by Circularly Polarized Light	265
9.4.3	Asymmetric Autocatalysis Triggered by Chiral Inorganic Crystals	265
9.4.4	Asymmetric Autocatalysis Triggered by Chiral Organic Crystals Composed of Achiral Organic Compounds	267
9.4.5	Spontaneous Absolute Asymmetric Synthesis	268
9.5	Conclusions	270
	Acknowledgment	271
	References	271
10	Recent Advances in Catalytic Asymmetric Desymmetrization Reactions	275
	<i>Tomislav Rovis</i>	
10.1	Introduction	275

10.2	Allylic Alkylation	276
10.3	Ring Opening of Epoxides and Aziridines	279
10.4	Ring Opening of Bridged Systems	284
10.5	Olefin Metathesis	289
10.6	Acylation	291
10.7	Asymmetric Deprotonation	294
10.8	Oxidations	296
10.9	Cyclic Anhydride Desymmetrization	300
10.10	Miscellaneous	303
10.11	Concluding Remarks	307
	Acknowledgments	308
	References	308
11	History and Perspective of Chiral Organic Catalysts	313
	<i>Gérald Lelais and David W. C. MacMillan</i>	
11.1	Introduction	313
11.2	Historical Background	315
11.3	Iminium Catalysis: A New Concept in Organocatalysis	319
11.4	Enamine Catalysis: Birth, Rebirth, and Rapid Growth	326
11.5	Brønsted Acid Catalysis: Hydrogen-Bonding Activation	331
11.6	Phase Transfer Catalysis (PTC)	335
11.7	Future Perspective	339
	Acknowledgments	340
	References and Notes	341
12	Chiral Brønsted/Lewis Acid Catalysts	359
	<i>Kazuaki Ishihara and Hisashi Yamamoto</i>	
12.1	Introduction	359
12.2	Chiral Brønsted Acid Catalysts	359
12.3	Chiral Lewis Acid Catalysts	363
12.3.1	B(III)	363
12.3.2	Al(III)	366
12.3.3	Ti(IV)	368
12.4	Lewis Acid-Assisted Chiral Brønsted Acid Catalysts	373
12.5	Conclusions and Outlook	379
	References	380
13	Chiral Bifunctional Acid/Base Catalysts	383
	<i>Masakatsu Shibasaki and Motomu Kanai</i>	
13.1	Introduction	383
13.2	Chiral Brønsted Base Catalysis	384
13.3	Chiral Brønsted Base–Lewis Acid Bifunctional Catalysis	386

13.4	Chiral Brönsted Base–Brönsted Acid Bifunctional Catalysis	392
13.5	Chiral Lewis Base Catalysis	394
13.6	Chiral Lewis Base–Lewis Acid Bifunctional Catalysis	397
13.7	Conclusion	404
	References and Notes	405
	Index	411

PREFACE

New Frontiers in Asymmetric Catalysis provides readers with a comprehensive perspective on understanding the concepts and applications of asymmetric catalysis reactions. Despite the availability of excellent comprehensive multivolume treatises in this field, we felt that researchers in pharmaceutical and chemical companies as well as university faculty and graduate students would benefit from a selection of some of the most important recent advances in this ever-growing area.

The key to efficient asymmetric catalysis lies in the creation of robust chiral catalysts by a suitable combination of chiral organic compounds and metal centers to which they are ligated. Many chiral organic ligands are *atropisomeric* (*a + tropos* in Greek) compounds with C_2 symmetry, such as BINOL and BINAP. The use of C_2 symmetric ligands originally introduced by Kagan had a strong impact on subsequent ligands design for asymmetric catalysis. In recent years new nonsymmetric ligands that are more effective than their C_2 counterparts have been reported. The first chapters of this book are dedicated to “rational” ligand design, which is critically dependent on the reaction type (reduction, oxidation, and C–C bond formation). The concept of C_2 symmetry for bidentate ligands can be extended to the design of C_n symmetric multidentate ligands bearing phosphorous, nitrogen, and other coordinating elements.

Catalyst systems can be described as biomimetic assemblies of multifunctional or bimetallic catalysts. Ideally, their design can be based on quantitative analysis of the transition state for a given reaction. Alternatively, a combinatorial screening of metal centers and chiral ligands can also lead to new catalyst systems. The development of efficient high-throughput screening methods for finding a good lead or an optimized catalytic system is still in its infancy.

In asymmetric catalysis, Sharpless emphasized the importance of “ligand-accelerated catalysis” through the construction of an asymmetric catalyst from an achiral precatalyst via ligand exchange with a chiral ligand. By contrast, a dynamic combinatorial approach, where an achiral precatalyst combined with several multicomponent chiral ligands (L^{1*} , — —) and several chiral activator ligands (A^{1*} , — —) may selectively assemble into the most active and highest enantioselective activated catalyst ($ML^{m*} A^{n*}$).

In Chapters 4–6, recent findings on activation of C–H bonds, C–C bonds and small molecules (C=O, HCN, RN=C, and CO₂) are covered. The latest developments on C–C bond reorganization such as metathesis (which earned the Nobel prize in chemistry, 2005) are also described.

Studies on the origin of chirality generated from achiral or racemic “primitive earth” provide the basis for asymmetric catalysis starting from racemic or achiral catalysts. Asymmetric catalysis through enantiomeric fluctuation or discrimination by an external chiral bias and subsequent amplification of chirality can be developed through autocatalysis with nonlinear effects. One strategy for achieving this enantiomeric discrimination is the addition of a chiral source, which selectively transforms one catalyst enantiomer into a highly activated or deactivated catalyst enantiomer. Recent progress on “chirally economical” nonlinear phenomena, racemic catalysis, and autocatalysis are highlighted in Chapters 7–9.

Asymmetric catalysis in target- or diversity-oriented synthesis becomes an increasingly important tool. Desymmetrization of symmetric intermediates (asymmetric or enantioselective desymmetrization) is one important synthetic strategy reviewed in Chapter 10. Use of naturally occurring enzymes is one of the oldest and most important approaches employed in asymmetric desymmetrization, the so-called classic mesotrick process. Generally effective methods for highly enantioselective aziridination of olefins, reduction and C–C bond formation of aliphatic ketones, are also expected to become practical (often via a pseudodesymmetrization process) in the very near future. Asymmetric catalytic tandem (domino) reaction sequences are likely to remain at the forefront of future research efforts.

Finally in Chapters 11–13, some of the more recent discoveries that have led to a renaissance in the field of organocatalysis are described. Included in this section are the development of chiral Brönsted acids and Lewis acidic metals bearing the conjugate base of the Brönsted acids as the ligands and the chiral bifunctional acid–base catalysts.

Although tremendous progress has been made in the field of asymmetric catalysis, very few systems have become widely applicable on an industrial scale because of challenges of catalyst efficiency (turnover number (TON) and frequency (TOF), catalyst loading, applicability to a wide range of systems and with feedstocks of varying purity and the levels of enantioselectivity). The best known are the Taka-sago menthol process, the Novartis imine hydrogenation for metolachlor, the Sumitomo cyclopropanation for cilastatine, and the Firmenich process of fragrant paradisone. For many asymmetric reactions, the recovery and recycling of the catalysts are a serious concern for both industry and society in order to limit the amount of waste, and impurities, that affect the overall costs of the processes.

Thus, the use of catalysts in new “green” reaction media such as ionic liquids, fluorous solvents, and supercritical carbon dioxide has become a viable alternative to those discussed within the chapters.

We hope that readers will find helpful and thought-provoking information in this book written by frontrunners in their respective fields, including the areas recognized by recent Nobel prizes in chemistry.

KOICHI MIKAMI

Department of Applied Chemistry Tokyo Institute of Technology

MARK LAUTENS

Department of Chemistry University of Toronto

December 25, 2006

CONTRIBUTORS

Kohsuke Aikawa, Department of Applied Chemistry, Tokyo Institute of Technology, Meguro-ku, Tokyo 152-8552, Japan

Tamio Hayashi, Department of Chemistry, Graduate School of Science, Kyoto University, Sakyo, Kyoto 606-8502, Japan

Kazuaki Ishihara, Graduate School of Engineering, Nagoya University, Furo-cho, Chikusa, Nagoya 464-8603, Japan

Henri B. Kagan, Laboratoire de Catalyse Moléculaire, Institut de Chimie Moléculaire et des Matériaux d'Orsay (CNRS UMR 8182), Université Paris-Sud, 91405-Orsay, France

Motomu Kanai, Graduate School of Pharmaceutical Sciences, The University of Tokyo, Hongo 7-3-1, Bunkyo-ku, Tokyo 113-0033, Japan

Tsuneomi Kawasaki, Department of Applied Chemistry, Tokyo University of Science, Kagurazaka, Shinjuku-ku, Tokyo 162-8601, Japan

Masato Kitamura, Department of Chemistry and Research Center for Materials Science, Nagoya University, Chikusa, Nagoya 464-8602, Japan

Gérald Lelais, Department of Chemistry, MC 164-30, California Institute of Technology, Pasadena, CA 91125, USA

Chao-Jun Li, Department of Chemistry, McGill University, 801 Sherbrooke Street West, Montreal, Quebec H3A 2K6, Canada

Zhiping Li, Department of Chemistry, McGill University, 801 Sherbrooke Street West, Montreal, Quebec H3A 2K6, Canada

David W. C. MacMillan, Department of Chemistry, MC 164-30, California Institute of Technology, Pasadena, CA 91125, USA

Koichi Mikami, Department of Applied Chemistry, Tokyo Institute of Technology, Meguro-ku, Tokyo 152-8552, Japan

Miwako Mori, Health Science University of Hokkaido, Ishikari-Toubetsu, Hokkaido 061-0293, Japan

Ryoji Noyori, Department of Chemistry and Research Center for Materials Science, Nagoya University, Chikusa, Nagoya 464-8602, Japan

Kyoko Nozaki, Department of Chemistry and Biotechnology, Graduate School of Engineering, The University of Tokyo, Hongo 7-3-1, Bunkyo-ku, Tokyo 113-8656, Japan

Takeshi Ohkuma, Division of Chemical Process Engineering, Graduate School of Engineering, Hokkaido University, Sapporo 060-8628, Japan

Tomislav Rovis, Department of Chemistry, Colorado State University, Fort Collins, CO 80523, USA

Itaru Sato, Department of Applied Chemistry, Tokyo University of Science, Kagurazaka, Shinjuku-ku, Tokyo 162-8601, Japan

Masakatsu Shibasaki, Graduate School of Pharmaceutical Sciences, The University of Tokyo, Hongo 7-3-1, Bunkyo-ku, Tokyo 113-0033, Japan

Ryo Shintani, Department of Chemistry, Graduate School of Science, Kyoto University, Sakyo, Kyoto 606-8502, Japan

Kenso Soai, Department of Applied Chemistry, Tokyo University of Science, Kagurazaka, Shinjuku-ku, Tokyo 162-8601, Japan

Tohru Yamada, Department of Chemistry, Keio University, Hiyoshi, Yokohama 223-8522, Japan (email: yamada@chem.keio.ac.jp)

Hisashi Yamamoto, Department of Chemistry, University of Chicago, 5735 South Ellis Avenue (SCL 317), Chicago, IL 60637, USA

1

LIGAND DESIGN FOR CATALYTIC ASYMMETRIC REDUCTION

TAKESHI OHKUMA

*Division of Chemical Process Engineering, Graduate School of Engineering,
Hokkaido University, Sapporo, Japan*

MASATO KITAMURA AND RYOJI NOYORI

*Department of Chemistry and Research Center for Materials Science,
Nagoya University, Chikusa, Nagoya, Japan*

1.1 INTRODUCTION

Molecular catalysts consisting of a metal or metal ion and a chiral organic ligand are widely used for asymmetric synthesis. Figure 1.1 illustrates a typical (but not general) scheme of asymmetric catalytic reaction.¹ The initially used chiral pre-catalyst **1A** is converted to the real catalyst **1B** through an induction process. An achiral reactant A and substrate B are activated by **1B** to form reversibly an intermediate **1C**. The chiral environment of **1C** induces asymmetric transformation of A and B to the chiral product A–B (*R* or *S*) through an intermediate **1D** with reproduction of catalyst **1B**. The absolute configuration of A–B is kinetically determined at the first irreversible step, **1C**→**1D**. The efficiency of catalysis depends on several kinetic and thermodynamic parameters, because most catalytic reactions proceed through such multistep transformation.

Catalytic asymmetric reduction of unsaturated compounds is one of the most reliable methods used to synthesize the corresponding chiral saturated products.^{2–4} Chiral transition metal complexes repeatedly activate an organic or inorganic hydride source, and transfer the hydride to olefins, ketones, or imines from one

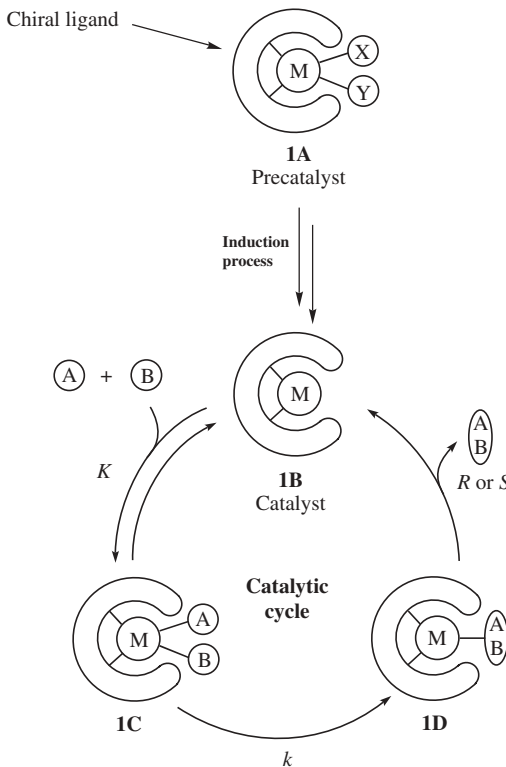


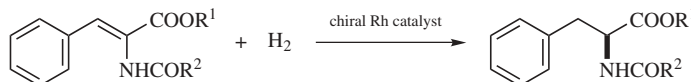
Figure 1.1. The principal of asymmetric catalysis with chiral organometallic molecular catalysts (M = metal; A, B = reactant and substrate; X, Y = neutral or anionic ligand).

of two enantiofaces selectively, resulting in the enantio-enriched alkanes, alcohols, or amines, respectively. The three-dimensional (3D) structure and functionality of the chiral ligand, among other factors, are the obvious key for efficient asymmetric reduction. Rational design of chiral ligand can be done on the basis of full understanding of the corresponding catalytic reaction. This chapter presents successful examples of catalytic asymmetric reduction and the concepts of the ligand design. The description is brought to focus on the BINAP–transition metal chemistry.²

1.2 HYDROGENATION OF OLEFINS

1.2.1 Enamide Hydrogenation with Rhodium Catalysts

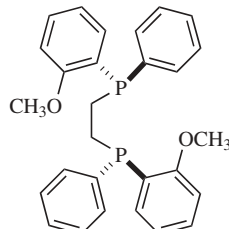
The discovery of Wilkinson complex, $\text{RhCl}[\text{P}(\text{C}_6\text{H}_5)_3]$,⁵ acting as an effective catalyst for hydrogenation of olefins opened the door for developing asymmetric reaction catalyzed by rhodium complexes with a chiral phosphine ligand.^{1,6–10} The enantioselective ability of chiral ligands has often been evaluated by hydrogenation of α -hydroxycarbonyl- or α -alkoxycarbonyl-substituted enamides. Figure 1.2



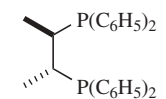
R^1 = H or CH_3

R^2 = CH_3 or C_6H_5

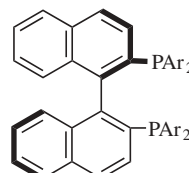
Examples of chiral ligands:



(*R,R*)-DIPAMP



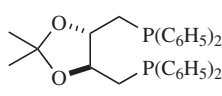
(*R,R*)-CHIRAPHOS



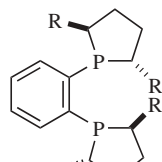
(*R*)-BINAP

BINAP: $Ar = C_6H_5$

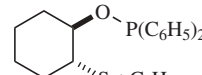
TolBINAP: $Ar = 4-CH_3C_6H_4$



(*S,S*)-DIOP

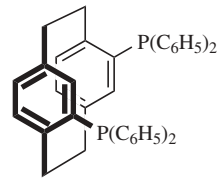
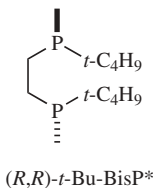


(*S,S*)-DuPHOS

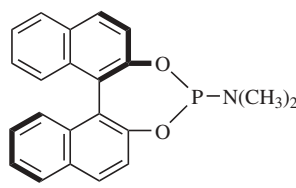


(*R,R*)-L1

Me-DuPHOS: $R = CH_3$
Et-DuPHOS: $R = C_2H_5$



(*S*)-[2.2]PHANEPOS



(*R*)-MonoPhos

Figure 1.2. Asymmetric hydrogenation of *N*-acylated dehydroamino acids and esters.

illustrates typical examples of phosphorus-based chiral ligands, with which Rh(I) catalyst selectively afforded (*S*)-amino acid derivatives in hydrogenation of (*Z*)-2-(acylamido)cinnamic acids and the methyl esters. Key factors for designing of these ligands are: (1) monodentate or bidentate, (2) steric effects (bulkiness, conformational flexibility, space coordinate, etc.), (3) electronic effects (alkylphosphine, arylphosphine, phosphite, phosphoramidite, etc.), (4) bite angle for bidentate

ligands, (5) C_1 or C_2 symmetry for bidentate ligands, and (6) chirality on the backbone or on phosphorus atoms. A DIPAMP–Rh-catalyzed hydrogenation of an enamide substrate is industrially used in the synthesis of L-dopa, a drug for the parkinsonian disease.⁸

The mechanism of hydrogenation of methyl (Z)-2-(acetamido)cinnamate catalyzed by a CHIRAPHOS¹¹ or DIPAMP–Rh⁸ complex have been exhaustively studied by Halpern^{12–14} and Brown.^{7,15,16} They proposed the “unsaturate/dihydride mechanism” as illustrated in Figure 1.3. The Rh complex with the *R,R* ligand $[(R)-3A]$ (solvate) and an enamide reversibly form the substrate complex **3B**, which undergoes irreversible oxidative addition of molecular H_2 to the Rh center, affording Rh(III) dihydride species **3C**. Both hydrides on Rh migrate onto the C–C double bond of the coordinated substrate. The first hydride migration to the C3 position forms a five-membered alkyl–hydride complex **3D**, and then reductive elimination of the hydrogenation product (second hydride migration) completes the cycle with regeneration of **3A**. The stereochemistry of product is determined at the first irreversible step, **3B** \rightarrow **3C**, although a detailed theoretical investigation suggests the possibility that the process **3B** \rightarrow **3C** is reversible and the step **3C** \rightarrow **3D** constitutes the turnover-limiting step.¹⁷ The BINAP–Rh-catalyzed hydrogenation of enamides is proposed to proceed with the same Halpern–Brown mechanism.^{18–21}

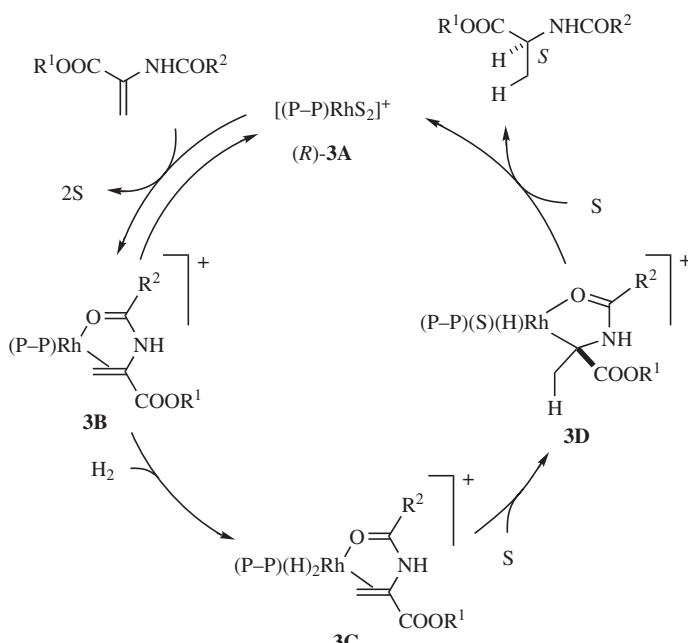


Figure 1.3. Catalytic hydrogenation of *N*-acylated dehydroamino esters via an unsaturated/dihydride mechanism; the β substituents in the substrates are omitted for clarity [$P-P = (R,R)$ -DIPAMP, (R,R) -CHIRAPHOS, or (R) -BINAP; S = solvent or a weak ligand].

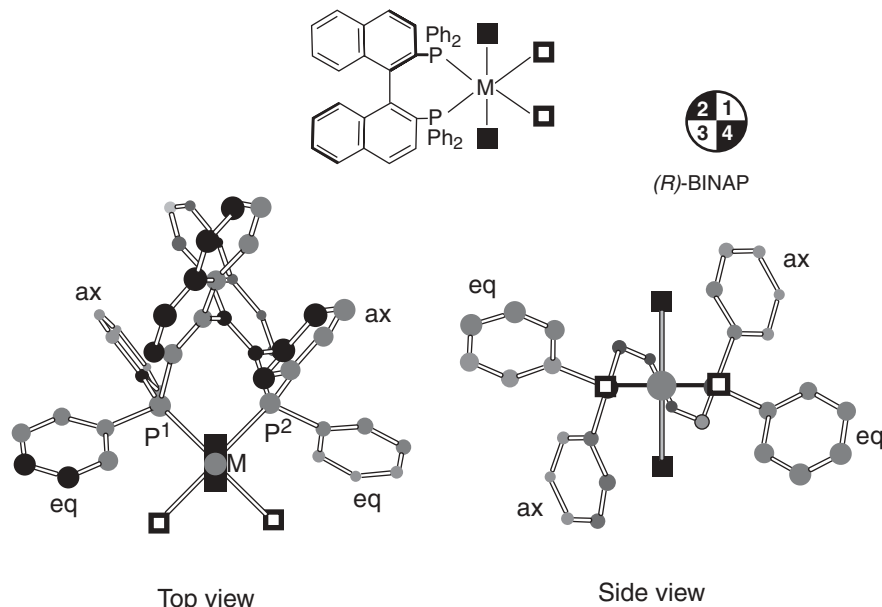


Figure 1.4. Chiral environment of an (R)-BINAP–transition metal complex (M = metallic element, ax = axial, eq = equatorial; □ = coordination site in the P^1 –M– P^2 plane; ■ = coordination site out of the P^1 –M– P^2 plane).

CHIRAPHOS, DIPAMP, and BINAP are all chiral diphosphines with a C_2 symmetry (Figure 1.2) forming chelate complexes with transition metallic elements. DIOP developed by Kagan is the origin of this type of chiral ligand.²² Figure 1.4 illustrates the chiral template created by an (R)-BINAP–transition metal complex.^{18–21} The naphthalene rings are omitted in the side view for clarity. In this template, the chiral information of binaphthyl backbone is transmitted through the P -phenyl rings to the four coordination sites shown by □ and ■. The in-plane coordination sites, □, are sterically affected by the “equatorial” phenyl rings, whereas the out-of-plane coordination sites, ■, are influenced by the “axial” phenyl groups. Consequently, the two kinds of quadrant of the chiral template (first and third vs. second and fourth) are clearly differentiated spatially, where the second and fourth quadrants are sterically congested, while the first and third ones are relatively uncrowded. (*R,R*)-CHIRAPHOS²³ and (*R,R*)-DIPAMP²⁴ form a similar chiral environment with metals.

As shown in Figure 1.3, the Rh catalyst (*R*)-3A and a bidentate enamide substrate reversibly form the substrate complex 3B. Figure 1.5 illustrates two possible diastereomeric structures of 3B, depending on the *Si/Re*-face selection at C2, which leads to the *R* or *S* hydrogenation product. Therefore, the enantioselectivity is determined by the relative equilibrium ratio and reactivity of *Si*-3B and *Re*-3B. A ^{31}P NMR spectrum of the Rh complex and an enamide substrate in CH_3OH showed a single signal for thermodynamically more favored *Si*-3B.²⁰ Most importantly,

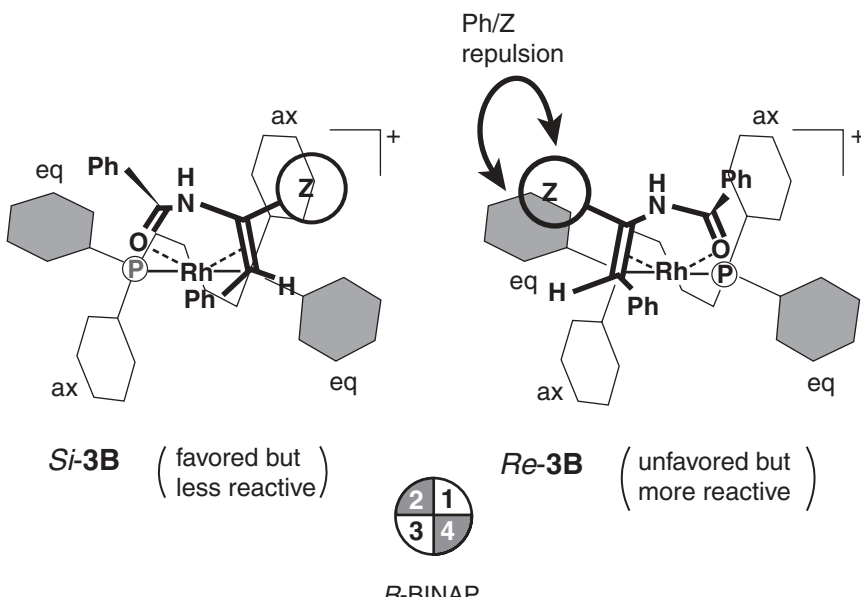


Figure 1.5. Molecular models of diastereomeric (*R*)-BINAP/enamide Rh complexes **3B** (not transition state) ($Z = \text{CO}_2\text{R}^1$; ax = axial, eq = equatorial).

the *Re*-**3B** which is less favored because of the nonbonded repulsion between an equatorial phenyl ring of the (*R*)-BINAP ligand and a carboxylate function of substrate reacts with H_2 much faster than the more stable *Si*-**3B**, leading to the *S* isomer as a major product. The observed enantioselectivity is a result of the delicate balance of the stability and reactivity of the diastereomeric **3B**. This inherent mechanistic problem requires careful choice of reaction parameters. For instance, the hydrogenation should be conducted under a low substrate concentration and low H_2 pressure to minimize reaction via the major diastereomeric intermediate *Si*-**3B**. Therefore, the hydrogenation of enamides catalyzed by BINAP-, CHIRAPHOS-, or DIPAMP-Rh complex, though giving amino acids in high enantiomeric excess (ee), is not ideal from the mechanistic standpoint. A Rh complex bearing Et-DuPHOS,²⁵ a C_2 -chiral diphosphines (see Figure 1.2), catalyzes the hydrogenation basically with the same mechanism.^{26,27}

This mechanistic problem can be solved when the more stable diastereomer of **3B** gives the major enantiomeric product. A Rh complex with a C_1 -chiral P/S mixed ligand, (*R,R*)-**L1** (see Figure 1.2), catalyzes hydrogenation of methyl (*Z*)-2-(acetamido)cinnamate to afford the *S* product in excellent ee.²⁸ The enamide substrate is reduced along with the catalytic cycle illustrated in Figure 1.3. However, unlike traditional catalyst systems, the stereochemistry of hydrogenation product suggests that the major *S* product is obtained via the most stable diastereomer of **3B**. A substrate complex, *Re*-**3B-L1**, is the only visible species among four possible diastereomers. Figure 1.6 illustrates the structure of an

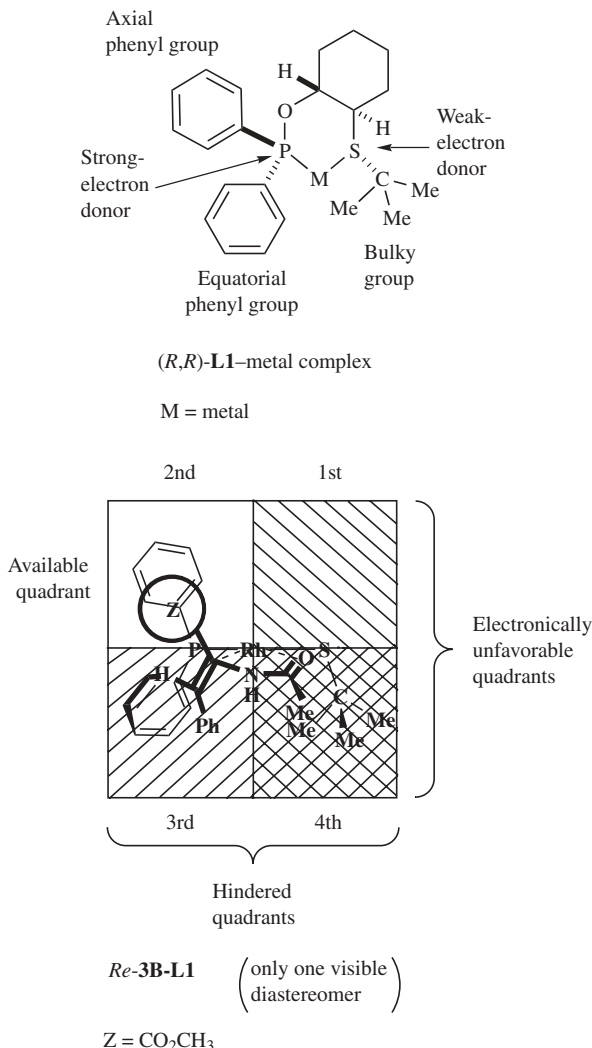


Figure 1.6. Molecular models of (R,R) -L1/enamide metal complexes.

(R,R) -L1–metal complex. The bulky *t*-butyl group on sulfur plays a crucial role in achieving high enantioface selectivity. This group is placed at the axial position to avoid steric hindrance with the ligand backbone. The two phenyl groups on phosphorus atom occupy the axial and equatorial positions. The high enantiodiscriminatory ability of the catalyst is rationalized by means of the quadrant model of *Re*-3B-L1.²⁸ The electron-donating olefin function of the enamide substrate preferably binds to Rh at the trans position to the less electron-donating sulfur atom instead of phosphorus, that is, the first and fourth quadrants are unfavorable for the olefinic function for electronic reasons. The third

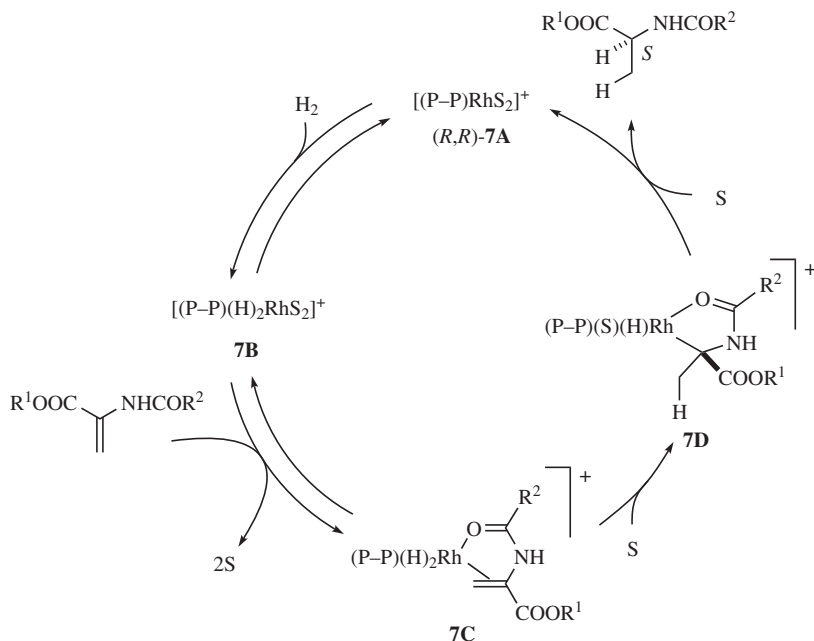


Figure 1.7. Catalytic hydrogenation of *N*-acylated dehydroamino esters via dihydride/unsaturate mechanism; the β substituents in the substrates are omitted for clarity [$\text{P-P} = (\text{R},\text{R})\text{-}t\text{-Bu-BisP}^*$; S = solvent or a weak ligand].

and fourth quadrants are blocked by equatorial *P*-phenyl and bulky *S*-*t*-butyl group, respectively. Therefore, only the second quadrant is available for approach of methoxycarbonyl group (*Z*).

The unsaturate/dihydride is not a sole mechanism for enamide hydrogenation. Its mechanistic problem can be resolved by a total change in catalytic cycle. *t*-Bu-BisP* is a C_2 -symmetric, fully alkylated diphosphine with chiral centers at phosphorus (see Figure 1.2).^{29,30} Hydrogenation of enamides catalyzed by an (*R,R*)-*t*-Bu-BisP*-Rh complex gives the *S* product in excellent ee. The hydrogenation is revealed to proceed through the “dihydride/unsaturate mechanism” as shown in Figure 1.7.³⁰⁻³² The major difference of this cycle from the unsaturate/dihydride cycle in Figure 1.3 is the order of reaction of the substrate and H_2 . Now the catalyst (*R,R*)-7A first reversibly reacts with H_2 , giving 7B, followed by interaction with an enamide substrate to form a substrate-RhH₂ complex 7C. The stereochemistry of product is determined at the first irreversible step, 7C \rightarrow 7D. Because of the C_2 -symmetric structure of (*R,R*)-*t*-Bu-BisP*, the quadrants of the chiral template are spatially differentiated into two kinds. The first and third quadrants are crowded by the location of bulky *P*-*t*-butyl groups, whereas the second and fourth ones are open for substrate approach owing to the presence of only small methyl groups. Therefore, two diastereomers of bidentate substrate-Rh(III)H₂ complex, *Re*-7C and *Si*-7C, are possible (Figure 1.8). Formation of *Si*-7C is

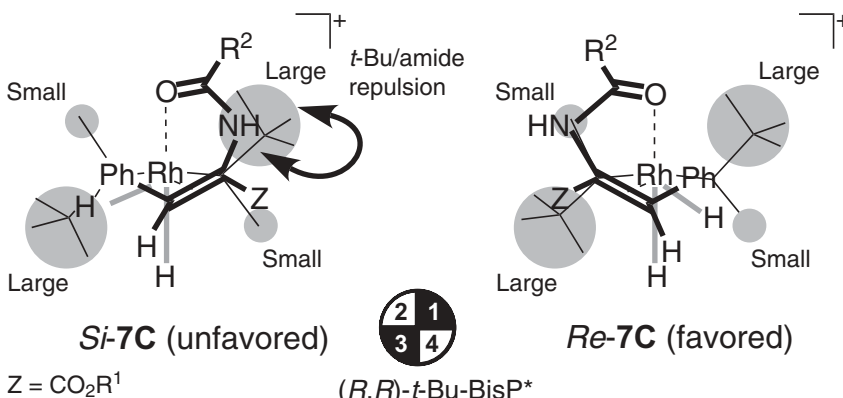


Figure 1.8. Molecular models of diastereomeric (R,R) -*t*-Bu-BisP*/enamide Rh complexes **7C** (not transition state).

unfavored because it suffers from serious steric repulsion between bulky *P*-*t*-butyl group and substrate amide function. On the other hand, only small methyl/amide repulsive interaction exists in *Re-7C*. The major *S* enantiomeric product is derived from the more stable diastereomeric species, *Re-7C*. The hydrogenation catalyzed by a [2,2]PHANEPHOS–Rh complex³³ (see Figure 1.2) is also suggested to proceed through the dihydride/unsaturated mechanism.³⁴

Chiral monodentate phosphites^{35,36} and phosphoramidites^{37,38} are also effective ligands for Rh-catalyzed asymmetric hydrogenation of enamide substrates. As seen in the structure of MonoPhos^{37,38} illustrated in Figure 1.2, combination of the modified BINOL backbone and the amine part gives a structural variety to this type of ligand.³⁹ Combinatorial methods are effective for optimization of the chiral structures.^{40,41} Elucidation of the hydrogenation mechanism catalyzed by the MonoPhos–Rh complex is in progress.^{42–44}

1.2.2 Hydrogenation of Functionalized Olefins with Ruthenium Catalysts

The BINAP–Rh catalyzed hydrogenation of functionalized olefins has a mechanistic drawback as described in Section 1.2.1. This problem was solved by the exploitation of BINAP–Ru(II) complexes.^{1,2} $\text{Ru}(\text{OCOCH}_3)_2(\text{binap})^{18}$ catalyzes highly enantioselective hydrogenation of a variety of olefinic substrates such as enamides, α,β - and β,γ -unsaturated carboxylic acids, and allylic and homoallylic alcohols (Figure 1.9).^{6,7,45–48} Chiral citronellol is produced in 300 ton quantity in year by this reaction.⁹

It is worth noting that an opposite sense of enantioface selection is observed in going from the BINAP–Rh complex to the Ru catalyst. Hydrogenation of methyl (*Z*)-2-(acetamido)cinnamate with the (*R*)-BINAP–Ru catalyst in CH_3OH gives the *R* (not *S*) product selectively (Figure 1.9).^{1,18,21,45} Figure 1.10 illustrates the

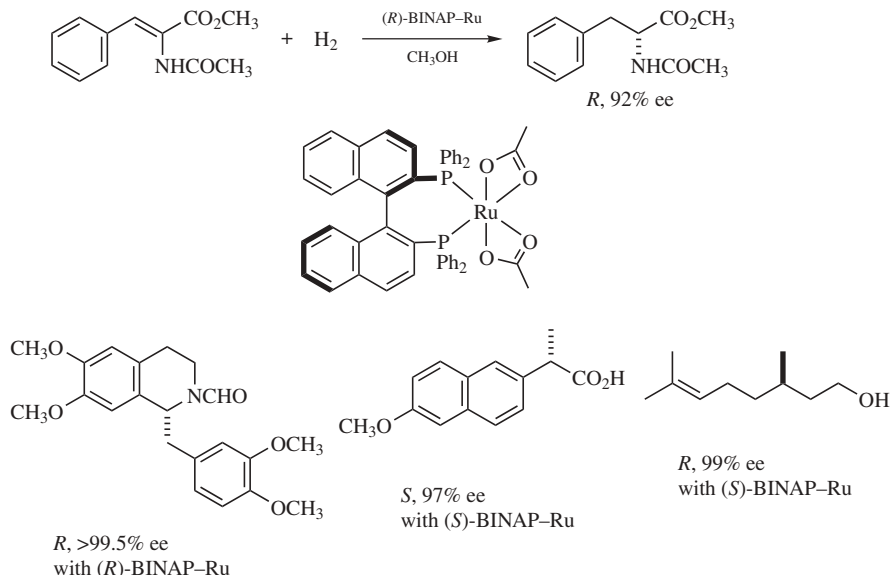


Figure 1.9. Asymmetric hydrogenation of functionalized olefins catalyzed by BINAP–Ru complexes.

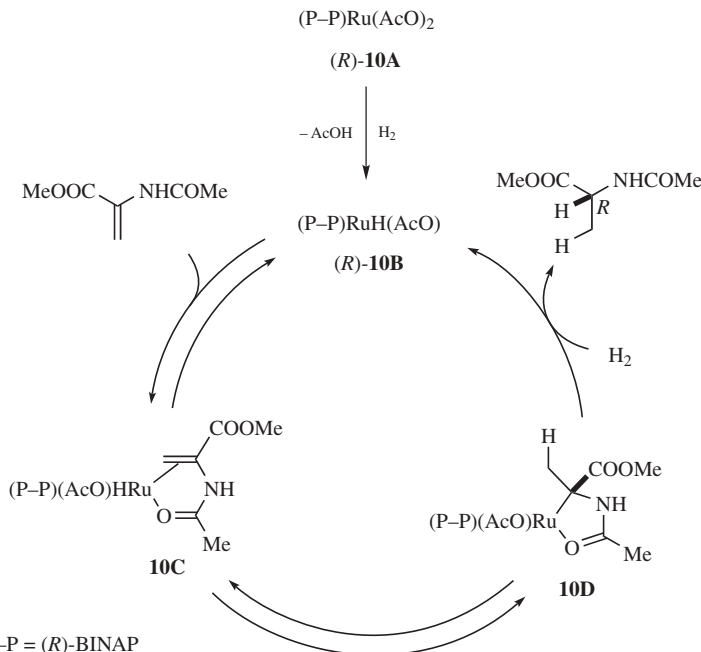


Figure 1.10. Catalytic cycle of BINAP–Ru-catalyzed hydrogenation of methyl (Z)- α -acetamidocinnamate involving a monohydride/unsaturated mechanism. The β substituents in the substrates are omitted for clarity.

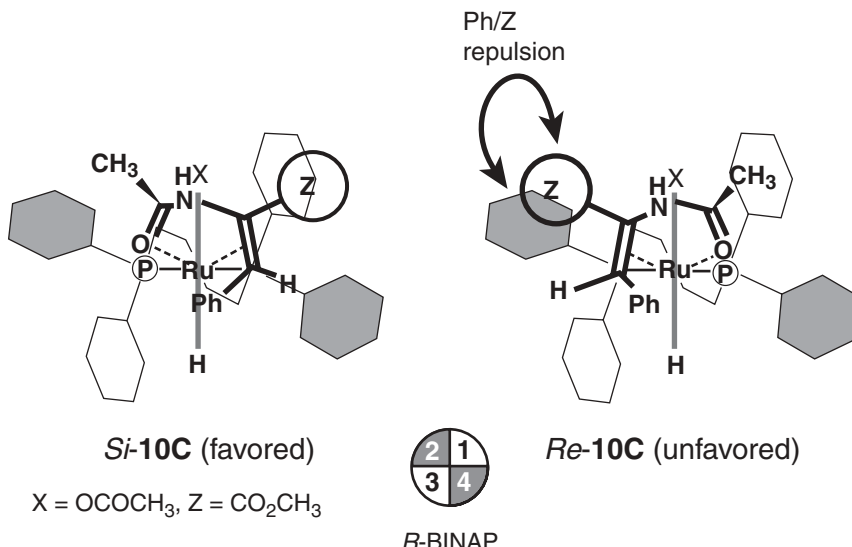


Figure 1.11. Molecular models of diastereomeric (*R*)-BINAP/enamide Ru complexes **10C** (not transition state).

“monohydride/unsaturate mechanism,” in which the $\text{RuH}(\text{AcO})$ species **10B**, formed by the heterolytic cleavage of H_2 by the precatalyst **10A**, acts as a real catalyst.^{21,49–53} Thus, the Ru hydride species is generated before the substrate coordination forming **10C**. The migratory insertion giving **10D**, in which the Ru–C bond is cleaved mainly by H_2 , but also by CH_3OH solvent to some extent. The irreversible step determines the absolute configuration of the product. Because the diastereomers of **10D** would have a similar reactivity, the enantioselectivity well corresponds to the relative stability of the diastereomeric substrate– $\text{RuH}(\text{AcO})$ complexes, *Re*-**10C** and *Si*-**10C** (Figure 1.11). In order for **10C** to undergo migratory insertion, the Ru–H and C2–C3 double bond must have a *syn*-parallel alignment. As discussed above, the intermediate *Re*-**10C** is unfavored relative to *Si*-**10C** because of existence of *P*-Ph/COOCH₃ repulsion. Therefore, the major *Si*-**10C** is converted to the *R* hydrogenation product through **10D**. The two hydrogen atoms incorporated in the product are from two different H_2 molecules, or H_2 and protic CH_3OH .

1.2.3 Hydrogenation of Simple Olefins with Iridium Catalysts

Phosphinodihydroxazole (PHOX) compounds, **L2–4**, act as P/N bidentate ligands showing excellent enantioselectivity in Ir-catalyzed hydrogenation of simple α,α -disubstituted and trisubstituted olefins (Figure 1.12).^{54–58} The use of tetrakis[3,5-bis(trifluoromethyl)phenyl]borate (BAr_F) as a counter anion achieves high catalytic efficiency due to avoidance of an inert Ir trimer

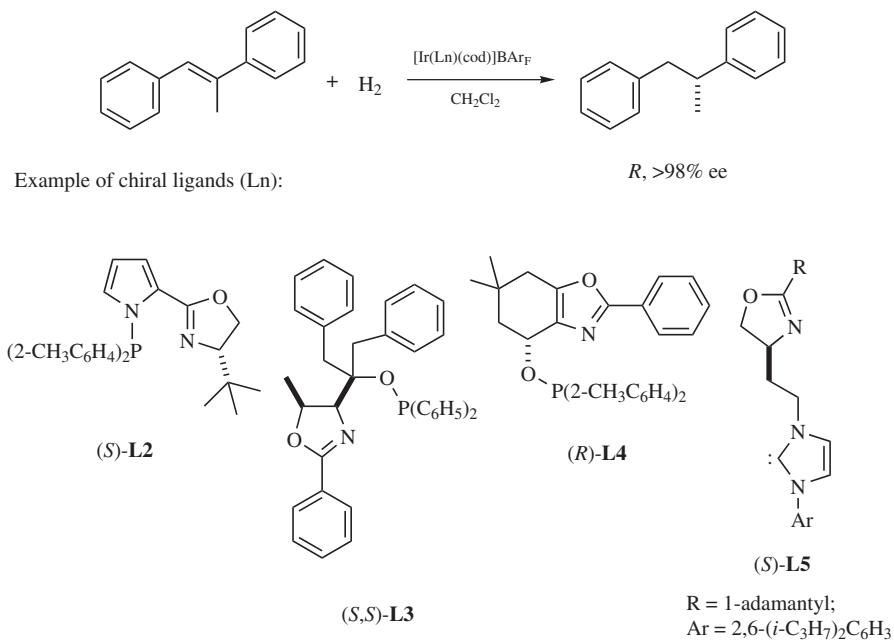


Figure 1.12. Asymmetric hydrogenation of simple olefins catalyzed by chiral Ir complexes.

formation. A chiral carbene–oxazoline ligand **L5** is also useful for this purpose.⁵⁹ The mechanism of this reaction is to be elucidated by experimental^{60–63} and theoretical^{64,65} studies. Chiral titanocene catalysts also show high enantioselectivity for hydrogenation of simple olefins.⁶⁶ This subject is discussed in Section 1.4.

1.3 REDUCTION OF KETONES

1.3.1 Hydrogenation of Functionalized Ketones

Although Ru(OCOCH₃)₂(binap) exhibits excellent catalytic performance on asymmetric hydrogenation of functionalized olefins, it is feebly active for reaction of ketones. This failure is due to the property of the anionic ligands. Simple replacement of the carboxylate ligand by halides achieves high catalytic activity for reaction of functionalized ketones.^{1,18,21,67} Thus, chiral precatalysts including RuCl₂[(*R*)-binap] (polymeric form),⁶⁷ RuCl₂[(*R*)-binap](dmf)_n (oligomeric form),⁶⁸ [RuCl{(*R*)-binap}(arene)]Cl,⁶⁹ [NH₂(C₂H₅)₂]₂[{RuCl{(*R*)-binap}}₂(μ -Cl)₃],⁶⁷ and other in situ formed (*R*)-BINAP–Ru complexes⁷⁰ are successfully used for hydrogenation of β -keto esters, resulting in the *R* β -hydroxy esters in >99% ee (Figure 1.13). An intermediate for the synthesis of carbapenem antibiotics is produced industrially by this method.¹⁸